Chemical characterization and reactivity of iron chelator-treated amphibole asbestos

Citation for the original published paper (version of record):

N.B. When citing this work, cite the original published paper.

(article starts on next page)

Chemical Characterization and Reactivity of Iron Chelator-treated Amphibole Asbestos

Julie Gold,[1] Helena Amandusson,[1] Anatol Krozer,[1] Bengt Kasemo,[1] Tore Ericsson,[2] Giovanna Zanetti,[3] and Bice Fubini[3]

[1]Department of Applied Physics, Chalmers University of Technology, Göteborg, Sweden; [2]Institute of Earth Sciences, Uppsala University, Uppsala, Sweden; [3]Department of Inorganic Chemistry, Chemical Physics, and Chemistry of Materials, University of Torino, Torino, Italy

Iron in amphibole asbestos is implicated in the pathogenicity of inhaled fibers. Evidence includes the observation that iron chelators can suppress fiber-induced tissue damage. This is believed to occur via the diminished production of fiber-associated reactive oxygen species. The purpose of this study was to explore possible mechanisms for the reduction of fiber toxicity by iron chelator treatments. We studied changes in the amount and the oxidation states of bulk and surface iron in crocidolite and amosite asbestos that were treated with iron-chelating desferrioxamine, ferrozine, sodium ascorbate, and phosphate buffer solutions. The results have been compared with the ability of the fibers to produce free radicals and decompose hydrogen peroxide in a cell-free system in vitro. We found that chelators can affect the amount of iron at the surface of the asbestos fibers and its valence, and that they can modify the chemical reactivity of these surfaces. However, we found no obvious or direct correlations between fiber reactivity and the amount of iron removed, the amount of iron at the fiber surface, or the oxidation state of surface iron. Our results suggest that surface Fe^{3+} ions may play a role in fiber-related carboxylate radical formation, and that desferrioxamine and phosphate groups detected at treated fiber surfaces may play a role in diminishing and enhancing, respectively, fiber redox activity. It is proposed that iron mobility in the silicate structure may play a larger role in the chemical reactivity of asbestos than previously assumed. — Environ Health Perspect 105(Suppl 5):1021–1030 (1997)

Key words: asbestos fibers, iron chelators, iron mobilization, free radical release, hydrogen peroxide, electron paramagnetic resonance spectroscopy, surface analysis, X-ray photoelectron spectroscopy, Mössbauer spectroscopy

Introduction

Iron in inhaled inorganic particulates may contribute to, or be the direct cause of, the pathogenicity of inhaled dusts and fibers. Both iron mobilized from the particulate and iron at the surface are implicated; the latter might also originate as iron redeposited from solution or endogenous sources (1–8). Many in vivo and in vitro investigations point to the crucial role played by free radicals and active oxygen

species in causing asbestos-mediated tissue damage (9–14). The highly reactive hydroxyl radical (·OH) has been invoked in many of these processes. Asbestos fibers can catalyze the production of free radicals, including hydroxyl radicals, in cell-free systems (15–18), in cell culture (14,19), and in vivo (12).

Asbestos-related free radical production, as well as biological damage, can be suppressed or inhibited by iron chelators, such as desferrioxamine and ferrozine, both when present in the test system and when used to pretreat fibers (17,20–24). On the other hand, other chelators such as ascorbate enhance free radical production (25). Chelators may remove iron from asbestos, alter iron valence states via oxidation or reduction, or remain bound at surface iron sites, thus preventing the participation of iron in redox reactions (15,26) or altering the overall redox potential of the asbestos fibers. In addition, chelators may stabilize iron that is released into the surrounding medium and thereby alter the dissolution kinetics. The mechanisms involved in the suppression of free radical production by iron chelator treatments have not been clearly elucidated. These mechanisms are key to understanding the specific role of iron and iron-catalyzed reactions in asbestos toxicity.

Much attention has been focused on the role of asbestos-associated iron in the production of hydroxyl radicals from H_2O_2 via catalytic Fenton and Haber-Weiss type reactions (15,17,22,27,28). Hydroxyl radicals are produced by the reduction of H_2O_2 by Fe^{2+} in the Fenton reaction, and by the reaction of H_2O_2 with superoxide anion (O_2^-) during the reduction of Fe^{3+} in the iron-catalyzed Haber-Weiss reaction. Another free radical of interest is the carboxylate radical ($CO_2^{-·}$), which is formed from the abstraction of hydrogen from formate ions ($HCO_2^{-·}$) on contact with the solid (17). Recent reviews by Hardy and Aust (29) and Fubini and Mollo (6) present a comprehensive overview of what is currently believed to be the role of iron in free radical production. A specific concern involves the influence and relative importance of Fe^{3+} and/or Fe^{2+} ions available for redox-cyclic reactions at fiber surfaces.

Within the amphibole asbestos group, crocidolite [$Na_2(Mg^{+2}, Fe^{+2})_3Fe^{+3}_2 Si_8O_{22}(OH)_2$] and amosite [$(Mg^{+2}, Fe^{+2})_7 Si_8O_{22}(OH)_2$] contain equivalent amounts of iron [27 and 28 wt%, respectively, as

determined for Union Internationale Contre le Cancer (UICC) asbestos (30)], but the iron is found in different valence states and crystallographic sites in these layered silicate structures. Iron in crocidolite is present in both 2^+ (≈ 55 atomic percent [at%]) and 3^+ (≈ 45 at%) valence states, while only the 2^+ state of iron is found within the amosite crystal structure. It is important to note that the majority of iron in the outermost atomic layers of both asbestos types is oxidized to Fe^{3+} (8,31), as expected. Cation lattice sites M1, M2, and M3 in these amphibole structures have octahedral coordination; M4 is a cubic site. Site population characterization indicates that the iron in amosite (as Fe^{2+}) is found in all cation sites. The Fe^{2+} ions in crocidolite are located in M1 and M3 sites, while Fe^{3+} ions are found in the M2 site (32).

Several methods have been employed to purposely alter surface Fe^{2+} and Fe^{3+} contents of fibers to study their influence on the redox reactions mentioned above. By far the most common technique involves the use of different iron chelators that specifically remove Fe^{2+} (e.g., ferrozine) or Fe^{3+} (e.g., desferrioxamine) ions or bind to these sites at the fiber surface. Asbestos surfaces have also been loaded with iron of a specific valence state by incubation in concentrated ferric or ferrous salt solutions (4,7). In both cases, the ability of silicates to catalyze DNA damage and generate oxygen radicals increased. Heat treatment in a reducing gas atmosphere is an effective method of producing Fe-reduced crocidolite with relatively long-term stability in air (10). Such a reduction treatment activated crocidolite fibers to enhance free radical production and lipid peroxidation. However, in the same study, Fe^{3+}-loaded crocidolite was shown to have a detoxifying effect. In general, it is clear that not all asbestos-associated iron is involved; it appears that the valence and location of iron in the lattice, as well as its availability for mobilization, control the activity of the fibers. Identification of the iron-binding sites responsible for fiber reactivity is yet to be determined.

The status of iron in asbestos is conventionally characterized indirectly by an analysis of how much iron can be removed from the fiber by valence-specific iron chelators. Similarly, iron concentration and valence state at chelator-treated surfaces are often described by how much iron of each valence state was removed from the fiber, rather than what actually remained at the surface. This description is questionable because surface reactions can rapidly change the valence state of an ion. Knowledge of what remains at the surface is particularly important, as interactions between fibers and the biological system occur or originate at this interface. For this and other reasons, it is important to characterize the iron that is actually present at the surface of native and iron-manipulated amphibole asbestos. By characterization of surface and bulk modifications induced by iron chelator treatments, it should be possible to better define the action of specific iron chelators and the role of iron in free radical production.

In this paper we report the use of X-ray photoelectron spectroscopy (XPS) and Mössbauer spectroscopy (MS) to characterize the nature of iron at the surface and in the bulk, respectively, of crocidolite and amosite asbestos when treated with desferrioxamine, ferrozine, sodium ascorbate, and phosphate buffer iron-chelating solutions. The effects of iron chelator treatments were then compared with the ability of the fibers to produce catalytic decomposition of H_2O_2 and generate free radicals, as determined in a cell-free system by the electron paramagnetic resonance (EPR) spin trapping method.

Methods

Fiber Preparation and Iron Mobilization

Samples of UICC crocidolite and amosite (33) in the nontreated, as received, condition were analyzed after incubation in one of the following iron-chelating solutions: desferrioxamine, sodium ascorbate, ferrozine, or phosphate buffer. Ascorbate is both a reducing agent and chelator: when Fe^{3+} is reduced to Fe^{2+}, the change in ion size facilitates its extraction from the silicate matrix. All solutions were prepared at 10-mM concentrations in water. Fibers were incubated at a concentration of 10 mg fibers/ml chelator solution for 3 days at 37°C and were continuously shaken and kept in the dark. No attempt was made to control pH. We believed that the pH should not change significantly during the incubation period, except for ferrozine, which most likely became acidic with incubation time. The use of buffer solutions can confound results, as buffers affect iron mobilization from crocidolite (34).

The fibers were centrifuged and the supernatants were filtered and analyzed for total iron content by atomic absorption spectroscopy (AAS) and inductively coupled plasma–atomic emission spectroscopy (ICP–AES) as a comparative technique. Fibers were rinsed in distilled water and vacuum dried for 48 hr at room temperature. A portion of each fiber type was packaged and stored under argon atmosphere until analyzed by XPS or MS (3 weeks–3 months). Another portion of fibers was retained for free radical and H_2O_2 decomposition testing and was stored in air for approximately 4 months prior to testing.

Characterization of Bulk and Surface Iron and Adsorbates

Mössbauer Spectroscopy. Characterization of the bulk iron in chelator-treated and nontreated asbestos fibers was performed by MS. The fibers were mixed with boron nitride and loosely packed into a metallic ring. In the transmission measurements, the angle between the normal of the absorber plane and the γ-direction was held at 54.7°, thus no texture effects were seen in the spectra (35). Accordingly, it was possible to fit the spectra using symmetrical doublets for Fe^{2+} and Fe^{3+} at the different crystallographic positions. The relative amount of ferrous and ferric iron was calculated from the areas of the doublets. This method assumes no sample thickness effects and equal f-factors at the different cationic binding sites.

X-ray Photoelectron Spectroscopy. XPS is a surface-sensitive analytical method in which analysis depth is limited to the top 5 to 10 atomic layers, or ≤ 10 nm. The detection limit of XPS is 0.1 to 1.0 at%, depending on the element. Changes in the surface chemical composition of amosite and crocidolite fibers due to chelator treatments have been evaluated with a PHI 5500C (Perkin-Elmer Corporation/Physical Electronics, Eden Prairie, MN) using a monochromatic Al Kα X-ray source with system spectral resolution approximately 0.5 eV [(31); Gold et al., in preparation]. Charge compensation was achieved by the use of low-energy electrons generated in an electron flood gun. A minimum of four analysis spots on one or more samples was used to calculate mean values of surface compositions.

To compare iron concentrations between samples, relative iron concentrations were used and were calculated by dividing the atomic concentration of iron (determined using the Fe 2p peak) by the atomic concentration of silicon (Si 2p). To determine the oxidation state of iron, semiquantitative evaluation of the high resolution Fe $2p_{3/2}$ photoelectron peak (obtained at 0.025 eV/step, 2.95 eV pass energy) was performed

by curve-fitting routines. This is necessary as there is insufficient resolution to distinguish the close-lying, multiplet-split peaks from Fe^{2+} and Fe^{3+} valence states. Curve-fitting procedures were developed to calculate the percentage of total iron in the Fe^{2+} or Fe^{3+} oxidation states [(31); Gold et al., in preparation]. Uncertainties in the curve fitting are inherently large, but we are able to follow trends that arise due to different chelator treatments.

Characterization of Fiber Reactivity

Free Radical Generation. EPR spectroscopy (Varian E109 EPR spectrometer [Varian, Palo Alto, CA] working in the X band [9–9.5 Ghz] with a double resonant cavity) was used to detect the formation of free radical species in aqueous suspensions of asbestos fibers via the spin-trapping method (16,17). The spin-trapping agent 5,5'-dimethyl-1-pyrroline-N-oxide (DMPO) forms stable radical adducts and was used to quantitate carboxylate and hydroxyl free radical release in solution. Two target molecules were used: sodium formate (F) and hydrogen peroxide 30% (P). They form the DMPO–COO·- and DMPO–·OH adducts, respectively. Each is characterized by a typical EPR spectrum. The intensity of the EPR signal is a measure of the number of radicals trapped by DMPO, and thus the number of radicals formed in the solution. These two tests are referred to as F–C (for carboxylate radical formation from the abstraction of a hydrogen atom from the formate ion) and P–OH (for hydroxyl radical formation from the decomposition of hydrogen peroxide via a Fenton mechanism or homolytic rupture), respectively.

In the F–C test, 45 mg of fibers was placed in 2 ml Chelex-treated 0.5 M phosphate buffer (Sigma Chemical, St. Louis, MO) (pH 7.4) containing 1 M sodium formate and 0.05 M DMPO. The suspension was incubated at 37°C and shaken in a dark reactor. Aliquots of the suspension were withdrawn at 55 min, then filtered and analyzed at room temperature approximately 5 min after the sample was withdrawn. The EPR spectrum was recorded at microwave power level 10 mW, scan range 100 G, and modulation amplitude 1 G. The spectrum shows six lines with intensity ratios 1:1:1:1:1:1, splitting constants $a_N = 15.2$ G, $a_H = 18.5$ G, and g-value = 2002.

In the P–OH test, the protocol is similar to that of the F–C test, but because of the lower DMPO adduct stability, incubation times are shorter. In this case, 45 mg of

fibers was placed into 2 ml solution consisting of 0.5 ml 0.5 M phosphate buffer (pH 7.4), 0.5 ml 30% H_2O_2 (diluted 1:50 in phosphate buffer), and 1 ml 0.05 M DMPO. The EPR spectrum was recorded after 30 min incubation. The spectrum shows four lines with intensity ratios 1:2:2:1, splitting constants $a_N = a_H = 149.9$ G, and g-value = 2054.

Because of an intrinsic variability from one DMPO preparation to another, blanks were performed in each set of experiments. Blanks were run with solution only (no asbestos fibers) and showed no radical formation. The intensity of the spectra was reported in arbitrary units calculated by dividing the height of the signal (in millimeters × 100) by the receiver gain.

Hydrogen Peroxide Decomposition. The percentage of H_2O_2 decomposed after 300 min incubation (37°C, shaken in dark reactor) of 50 mg treated or nontreated fibers with an H_2O_2 solution (1 ml 0.1 M H_2O_2 + 30 ml distilled H_2O) was determined by measuring the residual amount of H_2O_2 in 100 μl filtered suspension (17). Hydrogen peroxide was measured using an enzymatic assay whereby peroxidase catalyzes the oxidation of leuco crystal

violet by H_2O_2 via the method described by Mottola et al. (36).

Results

Iron Mobilization by Chelators

The total amount of iron mobilized from asbestos fibers into the chelator solutions was calculated on the basis of fiber weight or fiber surface and is shown in Figure 1A and B, respectively. Based on the theoretical composition and molecular weight of crocidolite and amosite, it was estimated that the amount of iron removed from the fibers due to chelator treatments was on the order of 1 to 5 at% of the total iron present in the fibers. The least amount of iron mobilized was found for the phosphate buffer solution. All other chelators mobilized between 2 to 4 times more iron, depending on whether iron removal is compared on the basis of weight versus surface area. Results obtained with the AAS and ICP–AES methods are comparable except in the case of ascorbate-treated crocidolite. The reason for this discrepancy is not clear.

Except for ferrozine treatments, slightly more iron could be mobilized
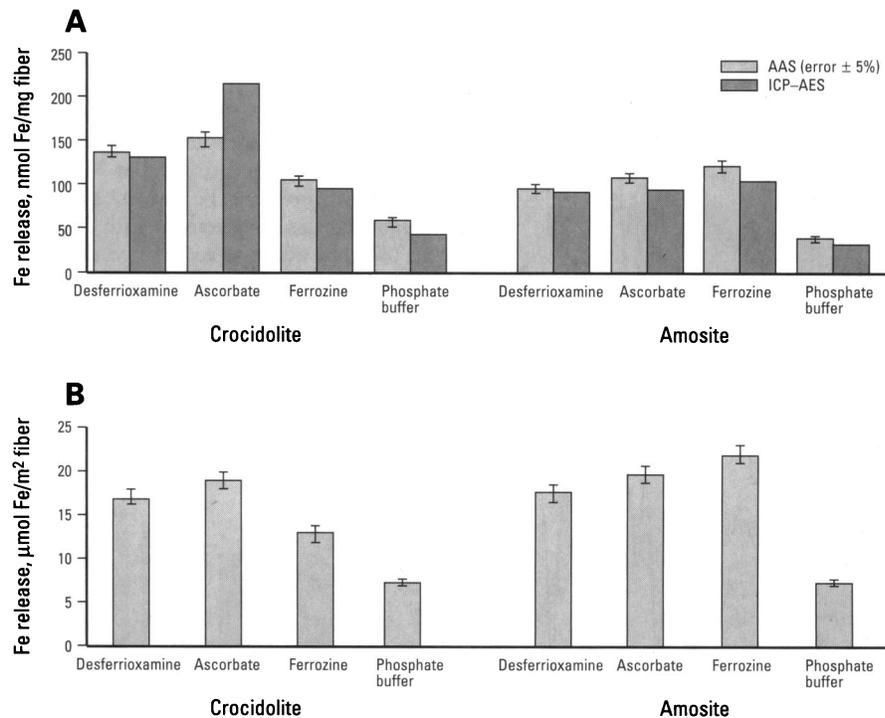

Figure 1. Total iron mobilized by desferrioxamine, ascorbate, ferrozine, and phosphate buffer from crocidolite and amosite, as determined by AAS and ICP–AES. (A) Iron release normalized by fiber weight. (B) Iron release normalized by fiber surface area (only AAS data presented). One set of measurements was made using each method. The error in the AAS measurement is estimated to be ±5%.

Table 1. Evaluation of Mössbauer spectra. Curve fitting parameters and resulting concentrations of iron ions in different cationic lattice sites in nontreated and chelator-treated crocidolite and amosite asbestos.

	Crocidolite			Amosite	
	D1	D2	D3	D1	D2
Doublet	1	2	3	1	2
Centroid shift[a] (mm/sec)	1.13	1.11	0.39	1.15	1.08
Quadrupole splitting[b] (mm/sec)	2.88	2.39	0.43	2.79	1.56
Lattice site	M1	M3	M2	M1, M2, M3	M4
Ion	Fe^{2+}	Fe^{2+}	Fe^{3+}	Fe^{2+}	Fe^{2+}
Relative concentration[c],%					
Nontreated	33.0	25.1	41.9	61.6	38.4
Desferrioxamine	30.6	29.7	39.6	63.4	36.6
Ascorbate	31.4	28.1	40.5	61.6	38.4
Ferrozine	31.9	26.8	41.3	60.9	39.1
Phosphate buffer	29.1	30.3	40.7	63.4	36.6

D, doublet. [a]Relative to metallic iron at room temperature. [b]Peak separation in the doublet. [c]Ratio of the area of the doublet to the total absorption area × 100%.

from crocidolite (surface area ≈ 8.3 m²/g) than amosite (surface area ≈ 5.7 m²/g) fibers for the same chelator treatment (Figure 1A), and this might be due to the greater surface area of crocidolite. If iron release is normalized by fiber surface area, as shown for the AAS data in Figure 1B, the amount of iron released from both fiber types is equivalent, again except for ferrozine. Ferrozine caused a significantly greater amount of iron mobilization from amosite than crocidolite.

Chemical Characterization of Asbestos

Bulk Iron. The results of the MS analysis reveal the distribution of bulk iron in the different cation lattice sites of the asbestos fibers (Table 1). An example of MS spectra obtained from crocidolite fibers is shown in Figure 2A. The room-temperature MS spectra of crocidolite were fitted by three doublets with centroid shifts ([CS] relative to metallic iron) and quadrupole splittings ([QS] peak separation in the doublet), as indicated in Table 1. The variation in these parameters was approximately ± 0.01 mm/sec between samples. The three doublets were assigned to Fe^{2+} at M1 sites, Fe^{2+} at M3 sites, and Fe^{3+} at M2 sites. The parameters are in agreement with Pollak et al. (37). In addition to the two doublets, there was also diffuse, broad absorption (not fitted, estimated to be a few percent of total signal) in the velocity range of 1.0 to 1.9 mm/sec (Figure 2A). Signal intensity in

this range was not affected by chelator treatments. This signal may emanate from iron close to or at the fiber surfaces, or from iron within the fibers in poorly defined locations.

The MS spectra of amosite (Figure 2B), also measured at room temperature, were fitted by two Fe^{2+} doublets with CS and QS as indicated in Table 1, again with a variation of approximately ± 0.01 mm/sec between the samples. These two doublets were assigned to iron in the M1, M2, and M3, and M4 crystallographic sites, respectively, as in earlier assignments (32). There was also a weak, nonfitted absorption in the interval 0.7 to 1.5 mm/sec that was not affected by the different chelator treatments.

Based on the results from Table 1, amosite was found to contain only Fe^{2+}, whereas crocidolite consisted of approximately 59 at% Fe^{2+} and 41 at% Fe^{3+}. Chelator treatments did not significantly affect bulk ferrous to ferric ratios.

Surface Composition. The primary elemental constituents detected by XPS at the surface (i.e., within approximately the top 10 atomic layers) of both treated and nontreated crocidolite and amosite fibers include O (≈ 40–50 at%), C (≈ 12–30 at%), Si (≈ 7–21 at%), and Fe (≈ 4–14 at%). Mg content of amosite surfaces (≈ 1–3 at%) was greater than crocidolite surfaces (typically < 1 at%), as can be expected from theoretical bulk compositions. Similarly, no Na was found on amosite surfaces, whereas 1 to 2 at% was detected on crocidolite. Low levels (typically ≤ 1 at%) of Ca, N, P, and K were also detected.

The amount of iron detected at the surface of the fibers as a function of chelator treatments is shown in Figure 3. The iron content has been normalized by the silicon content in order to preclude artifacts that might arise from compositional variations in other elements when samples are

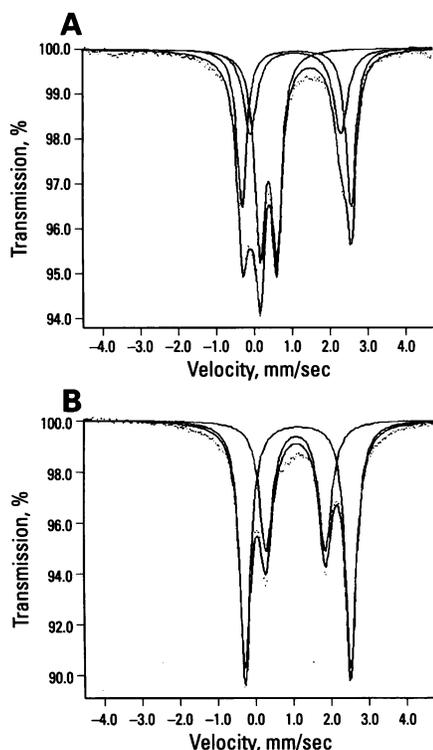**Figure 2.** Mössbauer spectra of nontreated (*A*) crocidolite and (*B*) amosite. Details of the doublet structures determined by curve fitting can be found in Table 1.
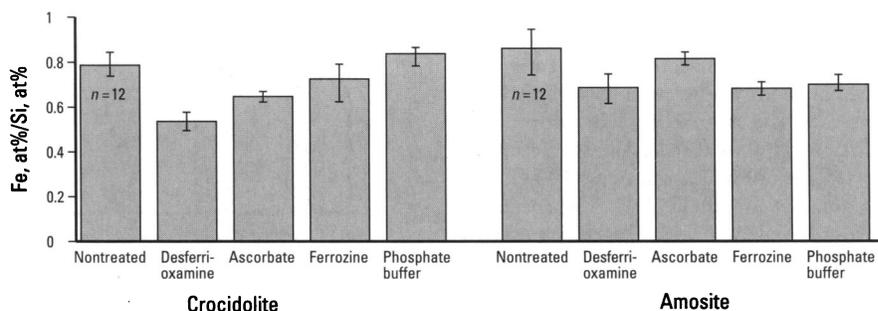

Figure 3. Relative surface iron content of nontreated and chelator-treated crocidolite and amosite, as determined by the ratio of the atomic concentration of iron (Fe 2p) to silicon (Si 2p) detected by XPS. Average values and standard deviations are shown.

compared. The Fe/Si ratio averaged approximately 0.8 for nontreated crocidolite and amosite surfaces.

Changes in surface iron content due to chelator treatments were observed; however, they differed for the two fiber types. For crocidolite, significantly lower iron concentrations were observed with desferrioxamine- (Fe/Si = 0.53) and ascorbate-treated (Fe/Si = 0.64) crocidolite surfaces compared to nontreated and phosphate buffer-treated crocidolite surfaces. However, there were no statistically significant differences in surface iron content between nontreated, ferrozine, and phosphate buffer-treated surfaces. For amosite surfaces, desferrioxamine, ferrozine, and phosphate buffer-treated fibers had lower iron content (Fe/Si ≈ 0.67) than non-treated fibers. However, there was no statistically significant difference in iron content of ascorbate-treated compared to nontreated amosite surfaces.

The oxidation states of iron present at fiber surfaces were determined by deconvoluting and curve fitting the Fe $2p_{3/2}$ photo-electron peak. An example of the curve fit is shown in Figure 4A for a spectrum obtained from nontreated crocidolite. (Details on the specific curve fitting procedure used can be found in Gold et al., in preparation.) Only Fe^{2+} and Fe^{3+} oxidation states were detected. Distinct differences in the Fe $2p_{3/2}$ peak shapes of nontreated crocidolite and amosite were observed (spectra not shown). These differences were expressed in the curve-fitting results shown in Figure 4B.

The most significant observation was that, despite the differing compositions of bulk iron between the two asbestos types, the majority of iron at all surfaces was in the Fe^{3+} state. There was on average approximately 5 at% more Fe^{2+} on nontreated amosite than crocidolite. This difference could be expected considering differences in Fe^{2+} content of their bulk compositions. It is surprising that not all surface iron is oxidized to the Fe^{3+} state, considering that these UICC samples were prepared almost 30 years ago and have been stored in air ever since (33). An average increase of 6 to 10 at% Fe^{2+} content was measured on chelator-treated amosite surfaces. There was a slight increase in Fe^{2+} on some ascorbate-treated crocidolite samples, but due to the large spread in the data, this increase was not statistically significant. The other chelator treatments did not alter the Fe^{2+} content of crocidolite surfaces.

Evidence of Adsorbed Chelators. Certain elements present in low quantities (≤ 1 at%) on the original asbestos were observed in larger quantities at the surface of chelator-treated fibers. The most significant findings include elevated levels of nitrogen on desferrioxamine-treated amosite and crocidolite, as can be seen in Figure 5. Although the levels are low and fall around 2 at%, they are significantly greater than the levels of nitrogen detected on all other surfaces, which fall around our estimated value for the detection limit of nitrogen on these surfaces (≈ 0.5 at%). Nitrogen generally adsorbs on surfaces from exposure to air, but in this
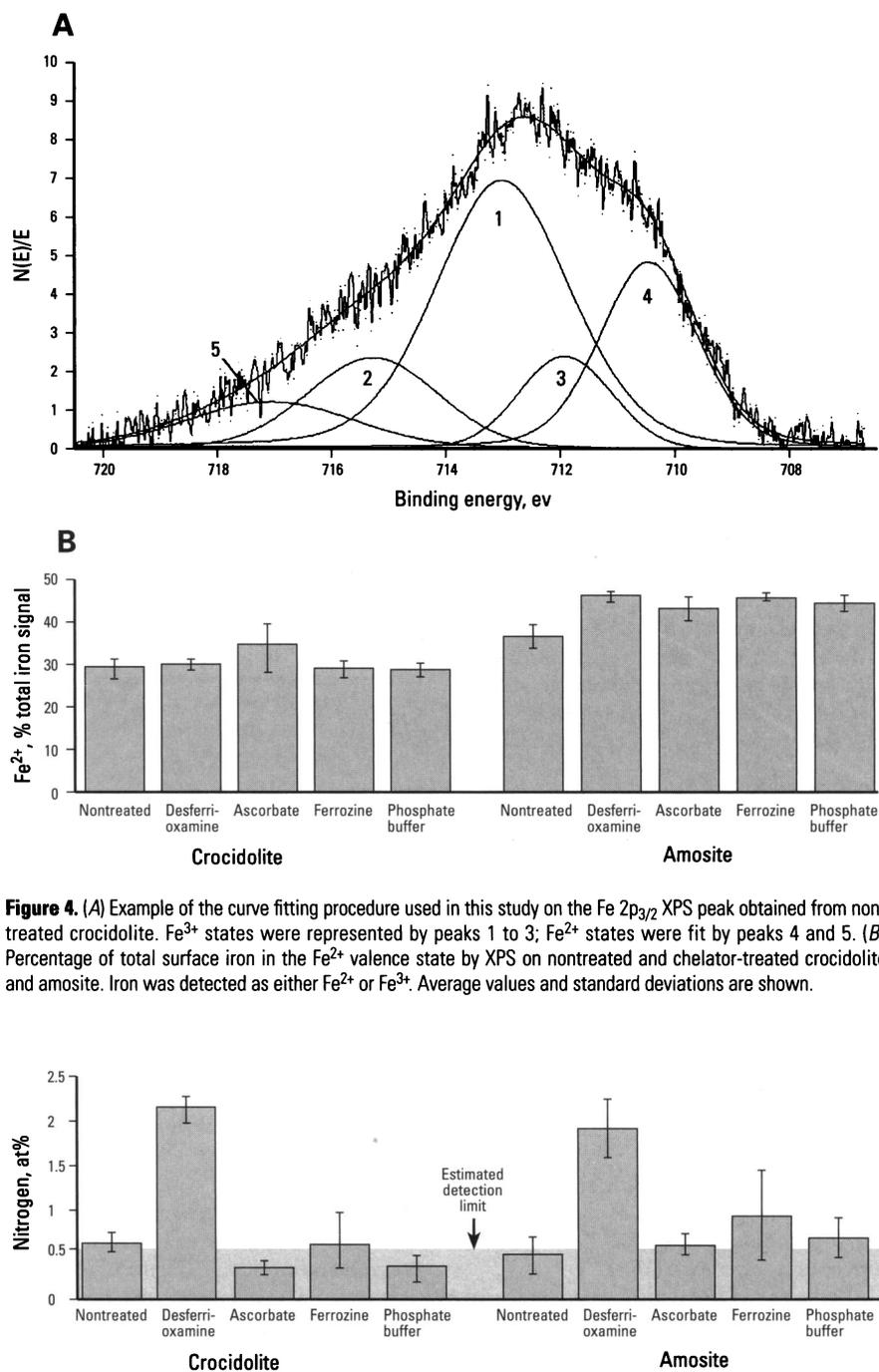
Figure 4. (A) Example of the curve fitting procedure used in this study on the Fe $2p_{3/2}$ XPS peak obtained from non-treated crocidolite. Fe^{3+} states were represented by peaks 1 to 3; Fe^{2+} states were fit by peaks 4 and 5. (B) Percentage of total surface iron in the Fe^{2+} valence state by XPS on nontreated and chelator-treated crocidolite and amosite. Iron was detected as either Fe^{2+} or Fe^{3+}. Average values and standard deviations are shown.

Figure 5. Evidence for desferrioxamine bound to crocidolite and amosite surfaces by nitrogen XPS spectra. Nitrogen concentration on desferrioxamine-treated fibers is elevated by approximately 1.5 at% compared to all other surfaces. Average values and standard deviations are plotted. The estimated detection limit for nitrogen on these samples (≈ 0.5 at%) is indicated.

study it probably also originates from adsorbed organic molecules such as the chelating molecules.

Additional evidence for desferrioxamine binding was found in the intensity and the binding energy position of the carbon 1s photoelectron peak. Specific differences were noted in the high-binding energy peak that typically appears as a shoulder in the C 1s spectra. The high-binding energy C 1s peak on crocidolite and amosite surfaces exposed to desferrioxamine was shifted by approximately 3.5 eV with respect to the main saturated hydrocarbon peak (≈ 285.6 eV), whereas on all other surfaces the shift was on average approximately 4.4 eV (crocidolite) or approximately 4.1 eV (amosite). In addition, the intensity of this high-binding energy C 1s peak tended to be higher on desferrioxamine-treated surfaces than on all other surfaces (data not shown).

Similar indications of phosphate bound to phosphate buffer-treated surfaces were observed by XPS analysis. Average concentrations of 0.8 to 1.2 at% phosphorus (as phosphate) and potassium were detected on phosphate buffer-treated surfaces, but were at or below the estimated detection limit for these elements (≈ 0.5 at%) on all other surfaces. Although these signals are small, with a wide spread in the data, we believe that this is evidence that phosphate remains adsorbed to phosphate buffer-treated fibers.

Redox Activity of Asbestos

Results from EPR spin trapping measurements, which detected the release of carboxylate (F–C test) and hydroxyl (P–OH test) free radicals are shown in Figure 6A and B and Figure 6C and D, respectively. It should be noted that the EPR signals have overall low intensities that are at or near detection levels. In fact, production of ·OH on nontreated amosite surfaces was below the detection limit. Low signal intensities are unavoidable, as both fibers are quite unreactive unless they are grounded. Nontreated crocidolite has slightly greater activity in both tests and generates more free radicals than amosite, but this could be an effect of the greater surface area for crocidolite.

Variations in free radical release potential following chelator treatments were observed on crocidolite and amosite for most chelators. All chelator treatments eliminated or reduced fiber reactivity in the F–C test (Figure 6A, B). This effect was most dramatic with amosite fibers (Figure 6A), as the DMPO–CO$_2^-$ signal was completely elimi-

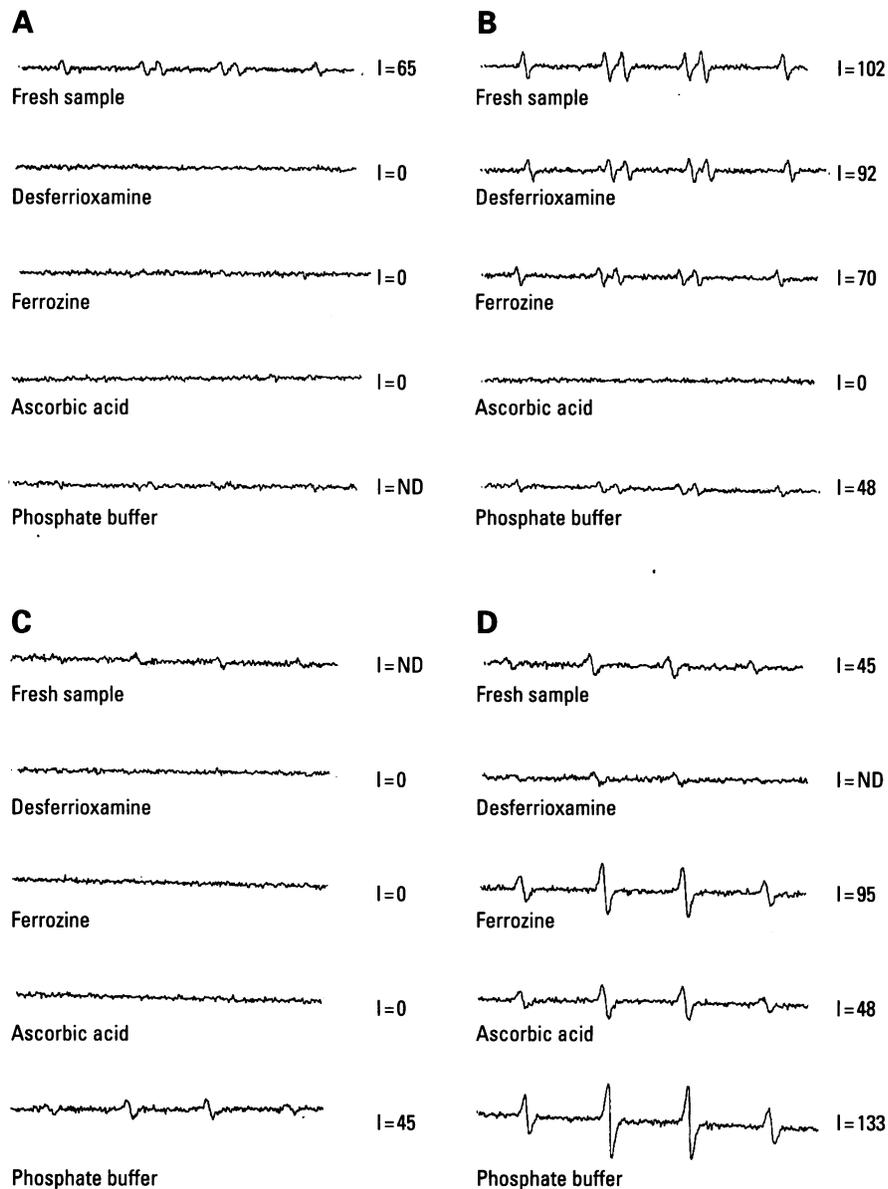**A**

B

C

D

Figure 6. Free radical release from amphibole asbestos showing the effect of chelator treatments on the potential for free radical release. EPR spectra of the DMPO–CO2$^-$ adduct collected during the F–C test are shown for (A) amosite and (B) crocidolite. EPR spectra of the DMPO–OH· adduct collected during the P–OH test are shown for (C) amosite and (D) crocidolite. The intensity of the EPR peak is proportional to the number of free radicals trapped. Abbreviations: I, intensity (arbitrary units); ND, nondetectable in the experimental conditions used.

nated with all chelator treatments. However, only ascorbate was able to eliminate CO$_2^-$· generation by crocidolite (Figure 6B).

Interesting results were obtained in the P–OH test (Figure 6C, D). Although ·OH was not generated by nontreated amosite fibers, incubation in phosphate buffer stimulated fiber activity to a level whereby DMPO–OH· could be detected (Figure 6C). Similarly, enhancement of the phosphate buffer was observed with crocidolite; the EPR

signal increased 3-fold over nontreated fibers (Figure 6D). Surprisingly, ferrozine also caused an increase in ·OH activity for crocidolite fibers. Desferrioxamine eliminated all ·OH release from crocidolite as expected; ascorbate caused no change in fiber activity.

Indication of the catalytic activity of asbestos fibers in the decomposition reaction of H$_2$O$_2$ was assessed by following the consumption of H$_2$O$_2$ in aqueous fiber suspensions. The results for nontreated and

chelator-treated fibers are shown in Figure 7A for crocidolite and Figure 7B for amosite. The H_2O_2 catalytic activity of both fiber types is decreased after chelator treatments, with the exception of ascorbate-treated amosite. Ferrozine treatments have the greatest reduction of fiber activity; desferrioxamine and phosphate buffer reduce the activity of both fibers by approximately one-half.

Discussion

Iron Mobilization by Chelator Treatments

Chelator treatments are responsible for the mobilization of iron from crocidolite and amosite: in the absence of chelators, no iron is removed from these fibers. As shown in Figure 1A, all chelators used in this study except ferrozine mobilized more iron from crocidolite than amosite fibers when compared on the basis of fiber

A

B

Figure 7. Catalytic decomposition of hydrogen peroxide by (A) crocidolite and (B) amosite and the effect of iron chelator pretreatments. The percentage of H_2O_2 decomposed after incubation for 300 min with nontreated or chelator-treated fibers is shown.

weight. However, when normalized by surface area, the two fiber types released similar amounts of iron, except in the case of ferrozine treatments. In this case, significantly more iron was mobilized from amosite than crocidolite. This can be expected, as ferrozine is Fe^{2+}-specific and amosite contains more surface and bulk Fe^{2+} ions than crocidolite. However, the corollary was not true: Desferrioxamine is Fe^{3+}-specific but did not remove more iron from crocidolite than amosite when compared on the basis of surface area. One explanation for this contradiction is that the chelator solutions were not buffered. Ferrozine becomes acidic under such conditions, whereas the desferroxamine solution is not as sensitive to the absence of buffer. The pH of chelator solutions can influence the solubility of iron and hence the amount of iron mobilized. It has been shown by Lund and Aust (34) that greater quantities of iron were mobilized by ferrozine at lower pH than neutral or basic pH. Because ferrozine only mobilizes Fe^{2+} ions, we observed more iron mobilized from amosite than crocidolite due to the larger reserve of Fe^{2+} in amosite. This would also be the case if Fe^{2+} ions were easier to remove from the silicate structure than Fe^{3+} ions.

The two analytical methods used to measure the total amount of iron in supernatant solutions give qualitatively similar results for different treatment solutions. The largest discrepancy occurs for ascorbate-treated crocidolite. Previous results also show larger amounts of iron released from ascorbate-treated crocidolite compared to other chelators (25). The general trend in iron release for different chelator solutions is in agreement with the literature after consideration of differences in incubation conditions (e.g., fiber and chelator concentrations, chelator solvent, pH, temperature, and time) (8,17,25,34).

Our estimation of the amount of iron removed during chelator treatments is on the order of 1 to 5 at% of the total iron present in the fibers. When the amount of iron removed per unit surface area, the number of unit cells per unit surface area, and the number of iron ions within each unit cell are considered, the iron removed from these asbestos fibers could have originated within one to a few unit cell layers below the surface. This estimation depends on how many iron ions were removed from each unit cell (assumed 50–100%). The depth of the surface modified region observed on desferrioxamine-treated crocidolite and amosite fibers by Mollo et al. (25), measured by high

resolution transmission electron microscopy (HRTEM), was on the order of 2 to 10 nm. Hence, this surface modified region could represent the depletion of iron, and possibly other M-site cations, from one to a few unit cell layers below the surface.

Iron Associated with Asbestos Fibers after Chelator Treatments

Chelator treatments did not affect the relative concentrations or lattice positions of Fe^{2+} and Fe^{3+} ions in the bulk of crocidolite and amosite fibers. Our average measurement of 59% of the total iron in crocidolite in the Fe^{2+} valence state is in agreement with expectations based on the theoretical composition ($\approx 55\%$). However, Pollak et al. (37) measured an Fe^{2+} concentration of only 46% on UICC crocidolite by MS. The reason for this disagreement is most likely due to their use of an extra doublet in the curve-fitting procedure around ± 1 mm/sec in the MS spectra, which was assigned to Fe^{3+} in the M1 lattice site. We could not fit an additional doublet in this region, perhaps due to a better signal-to-noise ratio in our data. We believe that iron contributing to the MS spectrum in this region probably resides at the surface of the fibers or in poorly defined lattice sites, or possibly originates from a highly mobile iron species, and cannot be clearly identified.

Because of the surface sensitivity of the XPS method, we were able to selectively probe the composition and binding states of elements only on the surface of the fibers. This corresponds to the modified surface region that was observed by Mollo et al. (25) after chelator treatments. It is not surprising that the iron content within the surface region is similar for nontreated crocidolite and amosite fibers, as their total iron contents are also similar to each other. However, the Fe/Si ratio of 0.8 measured in this and other recent studies (Gold et al., unpublished data) is significantly higher than the values of approximately 0.6 that we measured on the same fibers in previous years (31) and that were reported by Werner et al. (8). Different sample preparation and XPS analysis methods can explain this discrepancy (Gold et al., in preparation). Despite the higher Fe/Si ratio, we are still able to follow relative changes in Fe/Si ratio due to chelator treatments. Because the iron content is measured with respect to the silicon content, it is important to keep in mind that simultaneous and/or faster dissolution of the supporting silicate structure will clearly affect measurements of surface iron content by XPS, as postulated by Werner et al. (8).
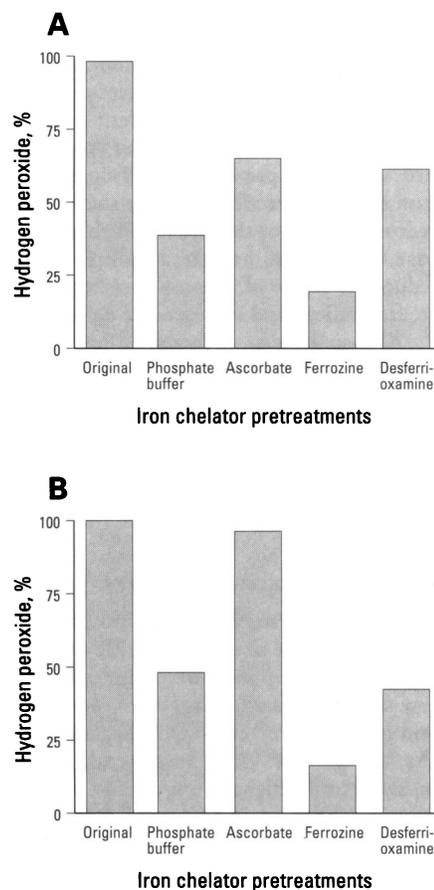
We measured reductions of up to 20 to 30% in relative surface iron content (Fe/Si ratio) on certain chelator-treated crocidolite and amosite fibers that were stored under inert atmosphere and for short time periods (3 weeks–3 months) after treatments. In some cases, the change in actual surface iron content may be larger or smaller due to possible differences between Fe and Si dissolution rates. Since relative surface iron content either decreased or remained unchanged, this is an indication that there is a net loss of iron from the fiber after most chelator treatments. This gives additional support to the claim that the modified region observed on desferrioxamine-treated asbestos surfaces by HRTEM (25) is a surface-depleted zone rather than a deposited surface film.

For ferrozine- and phosphate buffer-treated crocidolite, there was no reduction in surface iron content, despite the fact that iron was released into the chelating solutions. One explanation for this is that, in these two cases, iron ion diffusion from the bulk to the surface has occurred. Diffusion probably occurred in all chelator-treated crocidolite fibers and in amosite, but only in these two cases (which had the least iron release of the four chelators) was the initial surface concentration attained by the time of XPS analysis. Another explanation is that there was some reprecipitation of iron from solution to the surface, but not so much as to cause a net increase in surface iron content.

We would like to note here that in our previous studies, no changes in surface iron content were observed when chelator-treated fibers were allowed to age for long time periods (up to 1 year) in air prior to XPS analysis (31). It is known that oxygen-induced segregation takes place in metals. This suggests, again, the possibility of iron diffusion through the subsurface lattice at room temperature.

The majority of iron at both crocidolite and amosite surfaces is in the Fe^{3+} valence state, despite the fact that bulk concentrations of Fe^{2+} and Fe^{3+} determined by MS differ significantly for the two asbestos types. This agrees with the findings of Werner et al. (8) and is probably the result of oxidation of surface iron due to exposure to air both before and after chelator treatments. However, because our fibers were stored in an inert atmosphere prior to XPS analysis after chelator treatments, we were still able to detect differences in Fe^{2+} and Fe^{3+} concentrations at the fiber surfaces. In our previous studies of chelator-treated fibers stored in air (31), as in the study by Werner et al. (8), no significant changes in

surface iron oxidation states due to chelator treatments were observed.

Curve fitting of different valence states in the iron photoelectron peak is difficult and questionable due to overlapping multiplet split states for the Fe^{2+} and Fe^{3+} ions (31,38,39). However, it can be successfully used to follow changes in peak shapes due to chelator treatments, especially if comparisons with reference spectra are available. We observed significant increases of up to 10% in surface Fe^{2+} concentrations on chelator-treated amosite and ascorbate-treated crocidolite. We observed significant differences that followed the same trend with more than one curve-fitting routine (data not shown). However, changes in the oxidation state of surface iron due to chelator treatments did not correlate with the amount and type of iron assumed to have been removed from the surface. For example, ferrozine, which specifically chelates Fe^{2+}, mobilized the most amount of iron from amosite, yet the concentration of surface Fe^{2+} increased by almost 10% after treatment. A possible explanation for this is that Fe^{2+} reprecipitates onto the surface from the solution (although no evidence of the ferrozine molecule was detected) or that Fe^{2+} diffuses up to the surface from the subsurface region.

A comparison of Figures 1, 3, and 4 reveals no correlation between iron mobilization into chelator solutions and the amount and valence of iron remaining at the surface after chelator treatments. This agrees with results from Werner et al. (8), who concluded from similar types of experiments that it was not possible to correlate XPS results with iron mobilization data. The possibilities for rapid iron diffusion/migration to the surface, oxidation of surface iron due to exposure to ambient atmosphere, and simultaneous erosion of the silicate structure, complicate the analysis and do not allow such correlations to be made.

Detection of Adsorbed Chelators

Evidence for the adsorption of small quantities of desferrioxamine to crocidolite and amosite surfaces includes the following:

- A higher N content (1–2 at%) on desferrioxamine-treated surfaces. Nitrogen is a component of the desferrioxamine molecule and is part of the functional unit (hydroxamic acid) that binds to Fe^{3+} during chelation (40).
- The high-binding energy C 1s photoelectron peak has a peak shift of approximately 3.5 eV from the saturated hydrocarbon peak, which is smaller than

the peak shift observed on all other surfaces (≈ 4.2 eV). Organic carbon bound within a N—C=O type of environment would experience a binding energy shift between 3 to 4 eV, while carbon functional units such as O—C—O, O—C=O would shift typically between 4 and 4.5 eV (41). The latter is generally observed on oxide surfaces exposed to air. The observed change in peak shift on desferrioxamine-treated surfaces can be indicative of the presence of carbon bound in the N—C=O type of environment. This functional group also forms the active Fe^{3+} chelating center of the desferrioxamine molecule (40).

- The high-binding energy C 1s peak also has slightly greater intensity on desferrioxamine-treated surfaces compared to all other samples, which indicates the presence of a greater quantity of organic molecules on this surface than on the others.

Despite the fact that these XPS peaks have low intensity (1–2 at%), we feel that these three observations are significant and indicate that desferrioxamine molecules have adsorbed and remained adherent to fiber surfaces. Desferrioxamine bound at surface iron sites might prevent the participation of iron in redox reactions or alter the overall redox potential of the surface. If this is the case, desferrioxamine treatments would reduce the ability of asbestos fibers to generate free radicals and induce tissue damage.

XPS analysis has also shown low levels of phosphate adsorbed at phosphate buffer-treated fiber surfaces, either as reprecipitated iron phosphates or as surface adsorbed phosphate groups. We propose that this phosphate is associated with the elevated fiber activity observed in the production of ·OH from H_2O_2 in the P–OH test.

Catalytic Reactivity of Asbestos

The measurements of free radical production by asbestos fibers using EPR and the DMPO spin trapping method resulted in low signal intensities, as both crocidolite and amosite produce few radicals unless they are ground (17). In general, signal intensities were higher from crocidolite than amosite, and it could be argued that this is due to the larger surface area of crocidolite.

In the F–C test, it has been proposed that an oxidized surface site is reduced during the reaction [see Fubini et al. (17)]. In this study, all chelators decreased or eliminated ($CO_2^{-\cdot}$) production in the F–C test, as was also reported by Fubini et al. (17); this effect was most pronounced on all

treated amosite samples and on ascorbate-treated crocidolite. This could be related to the diminished quantity of oxidized iron sites at these surfaces (increased Fe^{2+} concentration), as measured by XPS analysis, which indicates that Fe^{3+} is used in the hydrogen extraction reaction with carboxylate. The usual effect of desferrioxamine, i.e., elimination of $CO_2^{-\bullet}$ release from crocidolite (17), was not observed. This might be due to the fact that, although the relative surface iron content was reduced, the relative amount of Fe^{3+} ions at the surface was not altered by chelator treatment (Figure 4B). Hence, there appears to be some correlation between the relative concentration of Fe^{3+} ions in the surface region and fiber activity in the F–C test.

In the P–OH test, it has been proposed that a reduced surface site is oxidized and drives the Fenton reduction of H_2O_2 to hydroxyl ion and hydroxyl radical (17). Phosphate buffer treatments enhanced the production of $\bullet$OH in the P–OH test for both asbestos types. This behavior is possibly influenced by the ability of adsorbed phosphates or precipitated iron phosphates to enhance reactivity. This seems likely, considering that phosphate strongly catalyzes the autoxidation of Fe^{2+} in solution (42). It is relevant to note that Fe^{2+} mobilization from crocidolite by ferrozine is prevented if phosphate buffer is used as the solvent but is not prevented if NaCl solution is used instead (34). Phosphate buffer might enhance hydroxyl radical production by enhancing the oxidation of Fe^{2+} to Fe^{3+} at asbestos surfaces. Note that phosphate buffer was present in both F–C and P–OH test solutions.

It is difficult to draw general conclusions about the effect of chelators on surface iron, the effects that changes in surface iron have on the catalytic reactivity of asbestos fibers, and the active sites responsible for fiber reactivity. For example, ferrozine treatments were most effective in diminishing H_2O_2 decomposition by crocidolite and amosite fibers; however, ferrozine-treated crocidolite fibers had twice as much $\bullet$OH release than nontreated fibers. It is clear that the catalytic decomposition of H_2O_2 does not coincide with $\bullet$OH (or $CO_2^{-\bullet}$) release, nor is it related to the surface iron content or its oxidation states. The activities found must be ascribed to iron present at the surface when these measurements were performed, assuming that iron is the active constituent of the mineral. We can conclude that fiber activity must be dependent on iron that has attained particular locations at the crystal surface, or

surface iron that has bound a chelator molecule (thus exhibiting a different redox potential), or on any iron that might have diffused from the near-surface region to the surface in the elapsed incubation time.

Summary

Under our experimental conditions, we estimate that 1 to 5 at% of the total iron contained in asbestos fibers was released into solutions of desferrioxamine, ascorbate, ferrozine, and phosphate buffer; iron mobilization was least in phosphate buffer solutions. There was no apparent correlation between the amount of iron mobilized by chelator treatments and the amount of iron remaining at fiber surfaces, which either decreased or remained unchanged compared to non-treated fibers. Although there was no significant change in the relative concentration of bulk Fe^{2+} and Fe^{3+} due to chelator treatments, the relative concentration of surface Fe^{2+} species increased on ascorbate-treated crocidolite and all chelator-treated amosite samples. Hence, iron mobilization data cannot be used to predict XPS results, and vice versa. However, XPS results have indicated that low levels of desferrioxamine and phosphate remained bound to both crocidolite and amosite surfaces.

Most, but not all, chelator treatments reduced the reactivity and catalytic activity of crocidolite and amosite asbestos. However, phosphate buffer treatments enhanced hydroxyl radical production by both crocidolite and amosite, as did ferrozine treatment of crocidolite. The usual effect of desferrioxamine, the elimination of free radical release from crocidolite, was not observed in the case of $CO_2^{-\bullet}$ generation. However, the interpretation of the free radical release data may be complicated by low signal intensities.

Our results indicate that Fe^{3+} is important for the hydrogen extraction reaction from carboxylate functional groups. No other correlations were found between iron mobilized by chelator treatments, iron detected by XPS at the treated surface, and the effect of iron chelators on chemical reactivity of crocidolite and amosite asbestos. We propose that iron mobility in the silicate structure may play a larger role in the chemical reactivity of asbestos fibers than previously assumed.

Conclusions

X-ray photoelectron spectroscopy has confirmed that iron chelators can modify the amount and valence states of iron at the surface of crocidolite and amosite

asbestos in addition to mobilizing iron from the fibers. However, we found no direct correlation between the amount of iron removed from fibers and changes in surface iron content (Fe/Si ratio). Observations could be complicated by: a) iron ion diffusion from the bulk to the surface, b) precipitation of iron complexes from the solution, and c) simultaneous dissolution of the supporting silicate structure. The valence state of iron found at chelator-treated fiber surfaces does not reflect the amount of Fe^{2+} or Fe^{3+} mobilized into solution, as assumed by the specificity of each chelator for iron in a particular oxidation state. This can be expected because of the reactivity of surface iron with oxygen when exposed to air, although it does not explain all of our observations. We cannot exclude the possibility of iron migration from subsurface layers and the precipitation of iron or iron complexes from the solution.

Few correlations were found between free radical release and H_2O_2 decomposition activities of iron chelator-treated fibers, and between these quantities and the amount of iron removed, the amount of iron remaining at the surface, and its oxidation state. Interpretations become complicated by adsorbed chelator species: Desferrioxamine and phosphate detected by XPS at fiber surfaces may play a role in diminishing and enhancing, respectively, iron activity in hydroxyl radical production. It is most likely that the catalytic activity of asbestos fibers is governed by several factors, such as iron mobility through the structure and the arrangement of iron ions at the surface, rather than the total quantity of iron at the surface and its oxidation state as analyzed by XPS.

REFERENCES

1. Lund LG, Aust AE. Mobilization of iron from crocidolite asbestos by certain chelators results in enhanced crocidolite-dependent oxygen consumption. Arch Biochem Biophys 287(1):91–96 (1991).
2. Lund LG, Aust AE. Iron mobilization from crocidolite asbestos greatly enhances crocidolite-dependent formation of DNA single-strand breaks in ϕX174 RFI DNA. Carcinogenesis 13(4):637–642 (1992).
3. Gulumian M, Bhoolia DJ, Theodorou P, Röllin HB, Pollak H, van Wyk JA. Parameters which determine the activity of the transition metal iron in crocidolite asbestos: ESR, Mössbauer spectroscopic

and iron mobilization studies. S Afr Tydskr Wet 89:405–409 (1993).

4. Ghio AJ, Kennedy TP, Stonehuerner JG, Crumbliss AL, Hoidal JR. DNA strand breaks following in vitro exposure to asbestos increase with surface-complexed (Fe^{3+}). Arch Biochem Biophys 311(1):13–18 (1994).

5. Lund LG, Williams MG, Dodson RF, Aust AE. Iron associated with asbestos bodies is responsible for the formation of single strand breaks in φ X174 RFI DNA. Occup Environ Med 51:200–204 (1994).

6. Fubini B, Mollo L. Role of iron in the reactivity of mineral fibers. Toxicol Lett 951:82–83 (1995).

7. Hardy JA, Aust AE. The effect of iron binding on the ability of crocidolite asbestos to catalyze DNA single strand breaks. Carcinogenesis 16(2):319–325 (1995).

8. Werner AJ, Hochella MF, Guthrie GD, Hardy JA, Aust AE, Rimstidt JD. Asbestiform riebeckite (crocidolite) dissolution in the presence of Fe chelators: implications for mineral-induced disease. Am Mineralogist 80:1093–1103 (1995).

9. Kamp DW, Graceffa P, Pryor WA, Weitzman SA. The role of free radicals in asbestos-induced diseases. Free Radic Biol Medicine 12:293–315 (1992).

10. Gulumian M, Bhoolia DJ, du Toit RSJ, Rendall REG, Pollak H, van Wyk JA, Rhempula M. Activation of UICC crocidolite: the effect of conversion of some ferric ions to ferrous ions. Environ Res 60:193–206 (1993).

11. Moyer VA, Cistulli CA, Vaslet CA, Kane AB. Oxygen radicals and asbestos carcinogenesis. Environ Health Perspect 102(10):131–136 (1994).

12. Schapira RM, Ghio AJ, Effros RM, Morrisey J, Dawson CA, Hacker AD. Hydroxyl radicals are formed in the rat lung after asbestos inst illation in vivo. Am J Respir Cell Mol Biol 10:573–579 (1994).

13. Gilmour PS, Beswick PH, Brown DM, Donaldson K. Detection of surface free radical activity of respirable industrial fibres using supercoiled φX174 RFI plasmid DNA. Carcinogenesis 16(12):2973–2979 (1995).

14. Kamp DW, Israbian VA, Preussen SE, Zhang CX, Weitzman SA. Asbestos causes DNA strand breaks in cultured pulmonary epithelial cells: role of iron-catalyzed free radicals. Am J Physiol 268:L471–L480 (1995).

15. Weitzman SA, Graceffa P. Asbestos catalyzes hydroxyl and superoxide radical generation from hydrogen peroxide. Arch Biochem Biophys 228(1):373–376 (1984).

16. Zalma R, Bonneau L, Guignard J, Pezerat H, Jaurand M. Formation of oxy radicals by oxygen reduction arising from the surface activity of asbestos. Can J Chem 65:2338–2341 (1987).

17. Fubini B, Mollo L, Giomello E. Free radical generation at the solid/liquid in iron containing minerals. Free Radic Res 23:593–614 (1995).

18. Fubini B. Use of physico-chemical and cell-free assays to evaluate the potential carcinogenicity of fibres. In: Mechanisms of Fibre Carcinogenesis (Kane AB, Saracci R, Boffetta P, Wilbourn JD, eds). IARC Sci Publ No 140. Lyon:International Agency for Research on Cancer, 1996 35–54.

19. Vallyathan V, Mega JF, Shi X, Dalal NS. Enhanced generation of free radicals from phagocytes induced by mineral dusts. Am J Respir Cell Mol Biol 6:404–413 (1992).

20. Weitzman SA, Weitberg AB. Asbestos-catalyzed lipid peroxidation and its inhibition by desferroxamine. Biochem J 225:259–262 (1985).

21. Turver CJ, Brown RC. The role of catalytic iron in asbestos induced lipid peroxidation and DNA-strand breakage in C3H10T1/2 cells. Br J Cancer 56:133–136 (1987).

22. Kennedy TP, Dodson R, Rao NV, Ky H, Hopkins C, Baser M, Tolley E, Hoidal JR. Dusts causing pneumoconiosis generate OH· and produce hemolysis by acting as Fenton catalysts.

23. Goodglick LA, Kane AB. Cytotoxicity of long and short crocidolite asbestos fibers in vitro and in vivo. Cancer Res 50:5253–5163 (1990).

24. Faux SP, Howden PJ, Levy LS. Iron-dependent formation of 8-hydroxydeoxyguanosine in isolated DNA and mutagenicity in Salmonella typhimurium TA102 induced by crocidolite. Carcinogenesis 15(8):1749–1751 (1994).

25. Mollo L, Merlo E, Giamello E, Volante M, Bolis V, Fubini B. Effect of chelators on the surface properties of asbestos. In: Cellular and Molecular Effects of Mineral and Synthetic Dusts and Fibers, Vol H85 (Davis JMG, Jaurand M-C, eds). Berlin/Heidelberg:Springer-Verlag, 1994;425–432.

26. Weitzman SA, Chester JF, Graceffa P. Binding of desferoxamine to asbestos fibers in vitro and in vivo. Carcinogenesis 9(9):1643–1645 (1988).

27. Graf E, Mahoney JR, Bryant RG, Eaton LW. Iron-catalyzed hydroxyl radical formation. J Biol Chem 259(6):3620–3624 (1984).

28. Pezerat H. Role of transition metal compounds in the capacity of dusts to generate electrophilic species. In: Cellular and Molecular Effects of Mineral and Synthetic Dusts and Fibers, Vol H85 (Davis JMG, Jaurand M-C, eds). Berlin/Heidelberg:Springer-Verlag, 1994;359–368.

29. Hardy JA, Aust AE. Iron in asbestos chemistry and carcinogenicity. Chem Rev 95(1):97–118 (1995).

30. Timbrell V. Characteristics of the International Union Against Cancer standard reference sample of asbestos. In: Pneumoconiosis: Proceedings of the International Conference, April 1969, Johannesburg, South Africa. (Shapiro HA, ed). Cape Town, South Africa:Oxford University Press, 1970; 28–36.

31. Amandusson H. XPS Analysis of Asbestos Fibers [M.S. Thesis]. Chalmers University of Technology, Gothenburg, Sweden, 1995.

32. Hawthorne FC. Crystal chemistry of the amphiboles. In: Amphiboles and Other Hydrous Pyriboles—Mineralogy, Reviews in Mineralogy, Vol 9A (Veblen DR, ed). Washington:Mineralogical Society of America, 1981;1–102.

33. Timbrell V, Rendall REG. Preparation of the UICC standard reference samples of asbestos. Powder Tech 5:279–287 (1971/1972).

34. Lund LG, Aust AE. Iron mobilization from asbestos by chelators and ascorbic acid. Arch Biochem Biophys 278(1):60–64 (1990).

35. Ericsson T, Wäppling R. Texture effects in 3/2–1/2 Mössbauer spectra. J Phys Coll 37:719–723 (1996).

36. Mottola HA, Simpson BE, Gorin G. Absorptiometric determination of hydrogen peroxide in submicrogram amounts with leuco crystal violet and peroxidase as catalyst. Anal Chem 42:410–412 (1970).

37. Pollak H, Waard Hd, Gulumian M. Mössbauer spectroscopic studies on three different types of crocidolite fibres. S Afr Tydsk Wet 89:401–404 (1993).

38. Brundle CR, Chuang TJ, Wendelt K. Core and valence level photoemission of iron oxide surfaces and the oxidation of iron. Surface Sci 68:459–468 (1977).

39. McIntyre NS, Zetaruk DG. X-ray photoelectron spectroscopic studies of iron oxides. Anal Chem 49(11):1521–1529 (1977).

40. Keberle H. The biochemistry of desferrioxamine and its relation to iron metabolism. Ann NY Acad Sci 119:758–768 (1964).

41. Beamson G, Briggs D. High Resolution XPS of Organic Polymers: The Scienta ESCA300 Database. Chichester, England:John Wiley & Sons, 1992.

42. Lambeth D, Ericson G, Yorek M, Ray P. Implications for in vitro studies of the autoxidation of ferrous ion and the iron-catalyzed autoxidation of dithiothreitol. Biochim Biophys Acta 719:501–508 (1982).

Arch Biochem Biophys 269(1):359–364 (1989).